Scientific Research Publishing

Journal of Applied Mathematics and Physics, 2025, 13(2), 575-592
https://www.scirp.org/journal/jamp
ISSN Online: 2327-4379
ISSN Print: 2327-4352

Beyond the Hertzsprung-Russell Diagram: An Enhanced Three-Dimensional Model Unveiling the Multidimensional Cosmos of Stars

Rohan Kumar

Frisco, TX, USA
Email: rohankumar.fb1@gmail.com

How to cite this paper: Kumar, R. (2025) Beyond the Hertzsprung-Russell Diagram: An Enhanced Three-Dimensional Model Unveiling the Multidimensional Cosmos of Stars. *Journal of Applied Mathematics and Physics*, **13**, 575-592.
https://doi.org/10.4236/jamp.2025.132032

Received: August 18, 2024
Accepted: November 5, 2024
Published: February 28, 2025

Abstract

Despite its utility in identifying patterns in celestial objects, the Hertzsprung-Russell diagram is not supported in dim or small stars; it struggles to provide insights into certain celestial objects such as brown dwarfs [1]. The purpose of this experiment is to create an improved version of the diagram with a three-dimensional model that includes a third z-axis to accurately predict and chart the life cycles of all stars regardless of size. The values of the stars' absolute magnitude and color indices were used to chart the surface gravity and metallicity, variables that were chosen due to their ease of collection and their likeliness to be within the range of values being assessed. To obtain the values for the model, data points from the database GAIA DR2 were utilized via the TAP protocol to query the SQL database. The data was transferred into a local CSV file to facilitate data manipulation. The data could be read and interpreted, as dim stars would likely have higher values of these variables, making it easier to include them in the diagram. The Pandas DataFrames tool on Python 3 was used to organize and manage the data efficiently. Matplotlib Graphs visualized the relationships between different stellar attributes by developing a linear regression line and an algorithm and creating scatter plots and sky maps to explore trends, hence designing three-dimensional diagrams. It was determined that the surface gravity diagram had a higher efficacy than metallicity due to their standard deviations of 0.4641441715272741 and 0.786577627976148, respectively.

Keywords

Color-Magnitude Diagram, Main Sequence, Metallicity, Spectral Energy Distribution Diagram, Surface Gravity, Three-Dimensional Stellar Evolution Models, Luminosity in Low-Mass Stars

1. Problem

The Hertzsprung-Russell diagram is an equation of stars' luminosity or absolute magnitude against their temperature or spectral class, and it was created by the U.S. astronomer Henry Norris Russell in 1911 and was based on the work of Danish astronomer Ejnar Hertzsprung. The diagram demonstrates patterns in stellar evolution, allowing one to see the path of a star throughout its lifetime, and therefore its luminosity, magnitude, and temperature throughout its lifetime [2].

One of the most remarkable contributions of the Hertzsprung-Russell diagram has been the establishment of Stellar Classification, a system that categorizes stars based on their spectral characteristics. This classification scheme has allowed astronomers to better understand the diversity of stars and study their individual properties in a systematic manner [3]. Moreover, the Hertzsprung-Russell diagram has been pivotal in the discovery and understanding of Stellar Evolution, the process through which stars undergo various stages of development over their lifetimes [4]. By observing the positions of stars on the Hertzsprung-Russell diagram, scientists can discern their evolutionary stage and make predictions about their future. The Hertzsprung-Russell diagram's most iconic feature is the Main Sequence, a diagonal band that represents the majority of stars in the universe (**Figure 1**). This sequence represents stars that are fusing hydrogen in their cores and serves as a benchmark for studying stellar populations [5]. It provides insights into the distribution and characteristics of stars in different regions of space. The Hertzsprung-Russell diagram has also been vital in identifying and studying Variable Stars, which exhibit fluctuations in brightness over time. By examining the

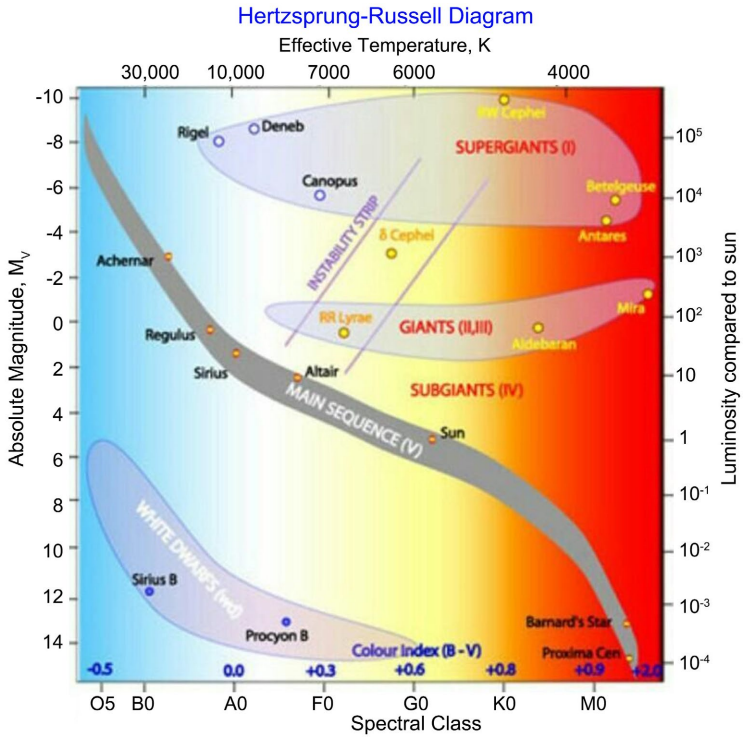

Figure 1. Normal Hertzsprung-Russell diagram.

positions of these stars on the diagram, astronomers have gained valuable information about their intrinsic properties and dynamics. Despite its immense contributions and utility in astronomy, the Hertzsprung-Russell diagram faces limitations, as there are some issues with the current diagram [6]. The diagram has faced challenges in accommodating certain celestial objects that do not fit neatly within its framework of spectral classes. One such example is the brown dwarf, a substellar object that falls below the temperature threshold of the Spectral Class M and, therefore, does not find a place on the Hertzsprung-Russell diagram. This discrepancy has led to inquiries about alternative models that can fill the gaps and propel the next age of scientific discovery.

2. Rationale

Currently, the Hertzsprung-Russell diagram is not supported in extremely dim and small stars, and the insights that it provides are limited to only two fields: magnitude and color index [7]. This research provides a significant value to the field of astronomy by seeking to help create another possible version of the Hertzsprung-Russell diagram that can provide useful insights not previously made available with the current diagram.

3. Variables

Controlled Variables: Number of Data Points, Range of the Study (0.5 - 2.5 solar magnitude for color index).

Independent Variable: Color Index.

Dependent Variable(s): Surface Gravity, Metallicity, Absolute Magnitude.

4. Engineering Goals

Inclusion Criteria: Systematic random sampling with a sample size of approximately 20,000 data points, with some invalidated due to mismatching IDs (19,786 data points were able to be used in the final product).

Exclusion Criteria: Data points of celestial objects with missing data, including variables such as no temperature or color index.

Of the goals present before experimentation, the first goal was to find out what stars are useful for the study by querying an astronomical database. After querying the database, another goal to be set to achieve can be to store this exported data locally for easier future reference.

Additionally, it should be ensured that the data is clear, clean, and precise by validating it and making sure that all of the values fall within a certain range, removing the possibility of large outliers that can skew the scale and the size of the finalized three-dimensional graph. Once the data has been sorted and cleaned, the final goal is to create a three-dimensional graph of the surface gravity and the metallicity values matched with each of the data points and star types, as well as a sky map (**Figure 2**) of the locations of all data points.

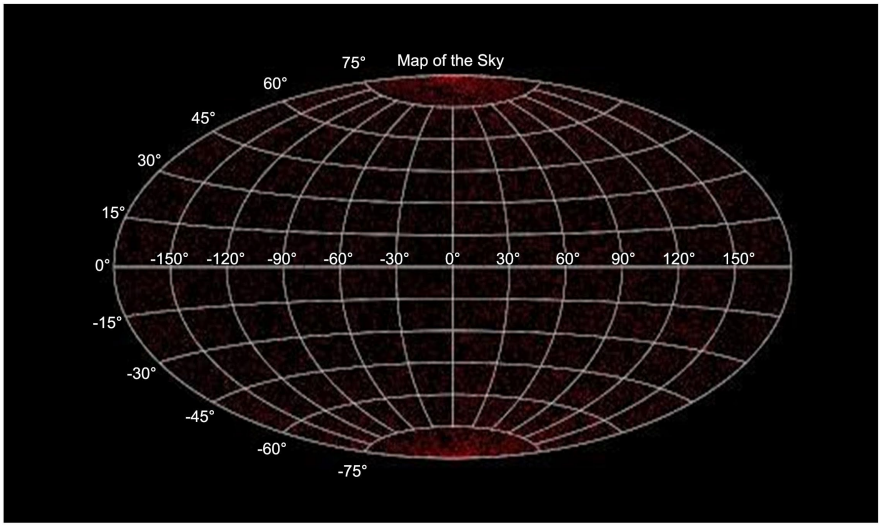

Figure 2. Sky map of points for newly-created 3D Hertzsprung-Russell diagram.

5. Research Question(s)

"What computational diagram can be developed to effectively supplant the Hertzsprung-Russell diagram and enhance its capabilities within the field of stellar classification and galaxy formation with a greater inclusiveness of celestial bodies, and what explanatory patterns can be observed from it?"

"How can a modified Hertzsprung-Russell diagram be used to find the relationship between surface gravity and metallicity with the color index using data analysis?"

6. Hypothesis

An expanded three-dimensional version of the Hertzsprung-Russell diagram, incorporating surface gravity and metallicity as possible third parameters, will address the limitations of the current diagram, which excludes certain stellar objects such as brown dwarfs. Moreover, surface gravity may serve as a more informative parameter in understanding stellar evolution across different types of stars.

7. Literature Review

A few research studies have endeavored to expand the traditional Hertzsprung-Russell diagram by incorporating a third dimension, often adding a z-axis to represent various stellar parameters.

These efforts aimed to enhance the understanding of stellar properties beyond the two-dimensional diagram. However, the parameters chosen in previous studies often failed to significantly enhance the diagram's predictive power or its applicability across a broader range of stellar types.

Previous attempts at a three-dimensional Hertzsprung-Russell diagram have included stellar age as a third parameter [8]. Research exemplified by Salaris and Cassisi explored the use of stellar age as the third axis in an attempt to enhance the Hertzsprung-Russell diagram's utility in studying stellar evolution. While this approach provided some insights into the life cycles of certain star types, it was limited

by the difficulties in accurately determining stellar ages and did not significantly improve the diagram's applicability to objects like brown dwarfs. Another attempt involves stellar mass as a third parameter, in which Torres *et al.* [9] introduced stellar mass as a third parameter, aiming to better categorize stars by their mass distribution.

However, the results showed that while mass is a critical factor in stellar evolution, it did not provide the necessary differentiation for stars that are similar in mass but vary greatly in other characteristics, such as temperature and luminosity.

In contrast to these earlier attempts, the current study is the first to integrate surface gravity and metallicity as third parameters in the diagram. These parameters were selected due to their strong correlation with a star's evolutionary stage and their ability to provide a more detailed understanding of stellar properties. The integration of surface gravity and metallicity into the Hertzsprung-Russell diagram allows for a more effective differentiation between stars of similar luminosity and temperature but at different evolutionary stages [10], which is particularly useful for categorizing stars like brown dwarfs and other celestial objects that are poorly served by the traditional Hertzsprung-Russell diagram. The surface gravity diagram adjusts the original diagram to include gravitational effects at a star's surface, providing insights into the structural integrity and evolutionary status of stars. Meanwhile, the metallicity diagram examines the abundance of elements heavier than hydrogen and helium, offering clues about the age and generation of stellar populations.

The findings indicate that the diagram incorporating surface gravity and metallicity outperforms previous models by offering a lower standard deviation and a higher coefficient of determination (R^2), making photometric systems a more precise and reliable tool for stellar classification [11]. This approach not only fills the gaps left by traditional and previous three-dimensional models but also sets a new standard for future enhancements of the diagram.

8. Expected Outcomes

The newly designed model of the Hertzsprung-Russell diagram that is to be designed will be able to accurately predict and chart the life cycle of all stars not included in the two-dimensional model, due to the presence of a z-axis. The new model should be able to have over 10,000 points at a single time and it should be able to be viewed from any angle without having performance issues. The graph should also be able to be viewed at any scale, and any point should be able to be zoomed in. It should be able to adjust to different parameters. It is expected that surface gravity and velocity are closely related to the color index and the star's magnitude [12]. The newly designed model of the Hertzsprung-Russell diagram should be able to accurately predict surface gravity due to the presence of a z-axis.

9. Computational Variables

The surface gravity of a star is the acceleration due to gravity experienced at the

outermost layer and is denoted by the symbol "g". It is measured in units of acceleration [Ex: centimeters per second squared (cm/s^2) or meters per second squared (m/s^2)].

Metallicity indicates an abundance of elements heavier than hydrogen and helium in a star. The metallicity of a star is represented by symbol "[Fe/H]".

The value [Fe/H] = 0 represents the metallicity of the Sun, and positive and negative values indicate higher and lower metal abundances, respectively.

Computational variables are observed through their spectral lines.

The relationship is between Mass and Radius: $g = GM/r^2$ (M is mass, r is radius, and M is the gravitational constant [6.67×10^{-11} newton]).

Surface Gravity = GM/r^2. "G" is the gravitational constant (6.67×10^{-17}). Using this equation, the mass and radius values were used to reverse engineer the surface gravity models as an additional form of data validation. As some of the radius values were roughly known, they were plugged into the equation to get the gravitational force or surface gravity.

10. Tools

Due to the computational and theoretical aspects of the research and experiment, no physical materials were required. However, many different computing resources were used to aid the research. First, the online database GAIA Data Release 2 was used, which is maintained by the European Space Agency [13]. The TAP protocol was used to query the database, which made it easy to change the data into a local CSV file that can be called and used more quickly than the database queries. Once the data had been compiled into a local CSV file, the Pandas DataFrames function and NumPy arrays were utilized to help specific data values be able to analyze more in detail and with ease. After using Pandas DataFrames, the Matplotlib library was finally used to first plot a normal Hertzsprung-Russell diagram and then create the two three-dimensional plots of the Hertzsprung-Russell diagram. All of the various functions were used to calculate the minimum mean and maximum of the data sets, as well as the standard deviations of the data sets (**Figure 3**). Linear regression lines, which utilize a form of artificial intelligence, were also used to help find the trends and create spreadsheets accordingly. Results are reproducible and consistent for anyone accessing the GAIA, HYG, and NED databases to retrieve surface gravity and metallicity values using Astroquery.

11. Data Collection

When querying the database, over 30 columns of data were present, out of which only 6 were used and over 24 were deleted, as they did not intrinsically relate to the study. In order to do this, the query had to be simplified to get only the columns that were pertinent to the study. The initial dataset was plotted on a preliminary three-dimensional diagram of the compiled data to ensure the dataset did not present any errors (**Figure 4**). After querying the databases, different numbers of results were

outputted for the star count. These data points were used to decide the range of surface gravity and metallicity to be used in the research.

2,552,168: Initial Dataset from GAIA 119,615: Dataset without null or zero values.

19,851: Final Dataset without negative values or mismatched IDs.

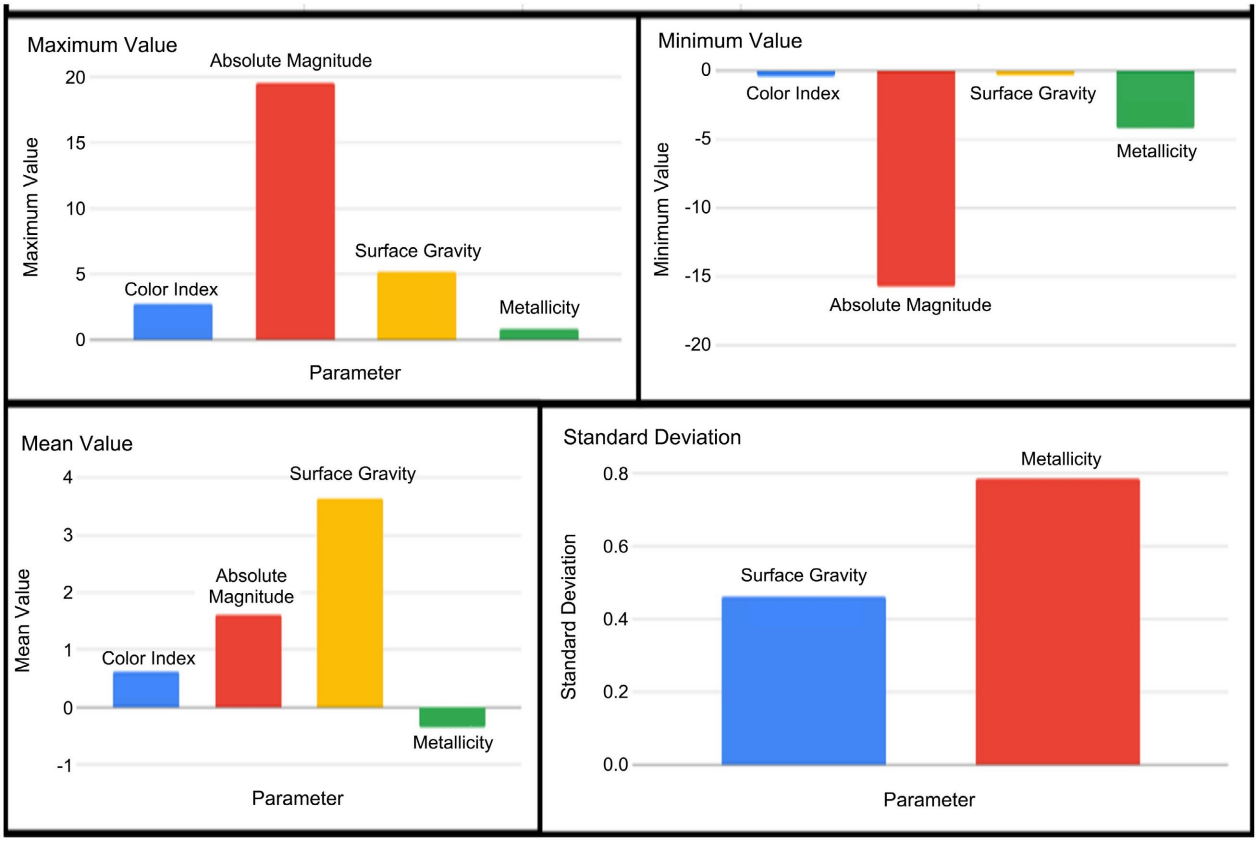

Figure 3. Graphical representation of precision measurements for surface gravity and metallicity.

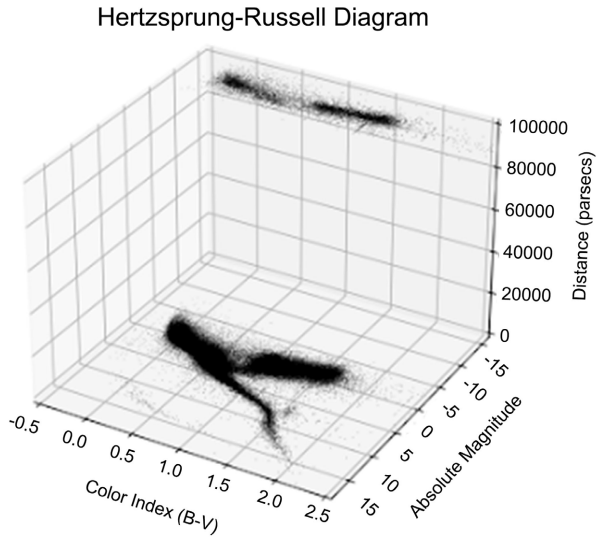

Figure 4. 3D Hertzsprung-Russell diagram of compiled data.

12. Risks and Safety

As the experimental phase is largely comprised of computational graph research and data analysis, there are minimal physical risks or hazards associated with this research. However, a few risks still exist regarding the safety of the digital environment in which the research is conducted. This includes potential data breaches or unauthorized access to information. Hence, safe practices were exercised. It was ensured that the data being downloaded was secure and that malware or files that could compromise the security of the database and computer were not being installed. Additionally, the risk of damaging the data set or losing important data while removing mismatching data points was present, as well as computer freezes while handling large amounts of data.

13. Implementations/Contributions

Increased Astronomical Knowledge: With an immense contribution to the field of astronomy, a greater utility of the Hertzsprung-Russell diagram will help the astronomical society better understand the correlation between metallicity and surface gravity for an increased number of stars.

Space Exploration Projects: By examining the distribution of stars within different regions of galaxies, galactic structure analysis from the Hertzsprung-Russell diagram with a wider range can also provide insight into information valuable for planning missions that involve the study of galaxies by aiding in mapping out the distribution of stars.

This research can also aid scientists' study of galaxy formation by making simulations with large datasets of stars more accurate due to their higher accuracy and inclusivity for trends in surface gravity. The increased accuracy of the surface gravity of the models is important due to its ability to make the stars more dynamic objects in the simulations by allowing them to have different gravities over the course of their lives, in addition to incorporating opacities [14].

The study of the surface gravity of a star is also important for determining the properties of the surrounding area of the stars, when a star with a higher metal content becomes a supernova, it can spread its metal contents across space, causing differences in the compositions of nearby nebula, which can thus lead to different metal compositions in the resulting stars, possibly changing their size and stellar properties.

14. Procedure

Background and Pre-Experiment Research: Research was conducted regarding the Hertzsprung-Russell diagram before experimentation. To address the issue of accommodating certain celestial objects into a diagram, background research before selecting the Hertzsprung-Russell diagram was conducted by exploring different models used to study stars. This included the Hertzsprung-Russell diagram, the color-magnitude (CMD) model, and the Spectral Energy Distribution (SED) diagram. In our comparative analysis, it was deduced that the Hertzsprung-Russell

diagram and the CMD model share similarities, both involving the plotting of luminosity (or magnitude) against temperature (or color). However, the CMD model focuses on incorporating the color index, which provides additional information about the star's temperature and intrinsic properties. In contrast, the Hertzsprung-Russell diagram focuses primarily on luminosity and effective temperature, making it a powerful tool for star classification, mass estimation, and understanding stellar populations and evolution. The SED diagram, on the other hand, offers a comprehensive view of a star's energy output across various wavelengths and allows researchers to study physical properties such as temperature, chemical composition, and stellar activity. However, constructing a SED diagram requires data spanning multiple wavelengths [15], posing challenges in obtaining accurate measurements. In light of our analysis, it was concluded that the Hertzsprung-Russell diagram remains the most effective overall comparative diagram for stars.

Querying of Data from GAIA, HYG, and NED: GAIA Data Release 2 was used to collect the most amount of data points for the stars out of the three databases due to its vast amount of publicly available data. The GAIA Data Release Two was utilized to access stellar data via the TAP protocol for querying astronomy data. This is achieved through querying the SQL database. The database was queried to extract relevant information, including luminosity, temperature/spectral type, mass, and age of stars. These additions unveiled useful patterns, and research on executing these steps was conducted in collaboration with our research guide at a university.

Data Preparation and Consolidation: The data was cut down slightly to make sure that all of the values matched to eliminate missing values. Upon querying the data, it was transferred into a local CSV file to facilitate data manipulation and analysis for reading and writing. Upon being able to read and write with the inputted data, certain observations regarding the stars will lower surface gravity were able to be made.

Graph Development of Surface Gravity and Metallicity: NumPy and Matplotlib were utilized to graph the values in three-dimensional models. The data from the CSV file was imported into Pandas DataFrames to organize and manage the data efficiently, and Matplotlib Graphs was utilized to visualize the relationships between different stellar attributes, creating initial scatter plots and histograms to explore distributions and trends. This helps create graphs and correlations between the different fields. The Python programming language NumPy was used to calculate the r values (correlation coefficients), or the values that correspond to how well the data correlates to a function, between various attributes, quantifying the degree of correlation between pairs of parameters.

Assessment of Experimental Design and Correlation: The surface gravity graph was found to contain the most accurate values for most stars due to having the lowest standard deviation, revealed through computational analysis. After finding the correlation coefficients for a variety of different attributes, they were evaluated to determine which has the highest r value, which helped identify the attributes that exhibit the strongest correlations. The attribute with the highest correlation

coefficient was then selected as the primary candidate to use for the expanded Hertzsprung-Russell diagram.

Calculations: The analysis was designed for robustness and reproducibility, beginning with the calculation of the color index from the B and V band magnitudes, a crucial indicator of stellar temperature. Surface gravity and metallicity indices were derived using established astrophysical formulas that relate these parameters to observable stellar properties, ensuring all methods were clearly referenced for accuracy. Statistical analysis involved correlation and regression models to examine the relationships between the color index and dependent variables—surface gravity, metallicity, and absolute magnitude. This approach allowed for precise predictions of these properties based on the color index variations. The results were analyzed to reveal how these indices interact, supporting the enhancements to the HR diagram and demonstrating their effectiveness in distinguishing different stellar types based on quantitative relationships. Creation of Regression Lines: After addressing the correlation analysis between surface gravity and metallicity, regression lines were created to find the correlation between a star's age and its metallicity (Figure 5). This can help astronomers to graphically view different solar systems and galaxies interacting over time. The slopes and r values of the linear regression lines were evaluated to determine the numerical correlation between surface gravity and metallicity, as well as evaluate the efficacy of the linear regression lines in reflecting the data from the three-dimensional models.

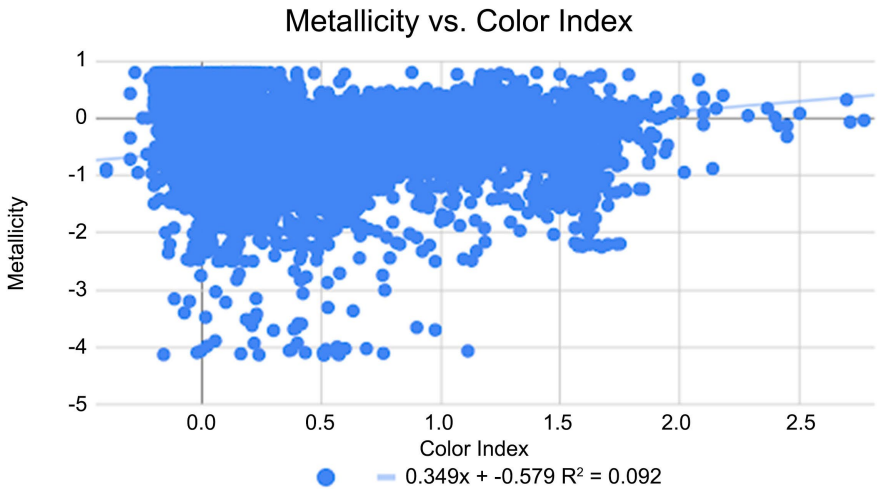

Figure 5. Regression line: metallicity vs. color index.

Procedure Overview: A three-dimensional Hertzsprung-Russell diagram was created, and this data in the form of a graph was attained through various inputs, including a CSV file, GAIA Database, and other consolidated information. The GAIA Database was initially used to query our data, using the TAP protocol [16]. The GAIA Database is a database that is maintained by the European Space Agency, and its most recent update, Data Release 2 in 2020, provided the most updated information that the research strategy would need. In the collection of the data, the TAP protocols were used to query the data from the server. TAP protocols are an

astronomical query format that many online databases accept, and the protocols were used to query the GAIA Data Release 2 to find the color index, the surface gravity, metallicity and the absolute magnitude. Additional data regarding the galactic latitude and the galactic longitude were also collected. The Python Astroquery library was used to help query the database in a faster method and to add it to a Comma Separated File, or CSV file. Inputting the data into a CSV file facilitated the ease of accessing the data, rather than having to call the GAIA Database for thousands of items during each adjustment.

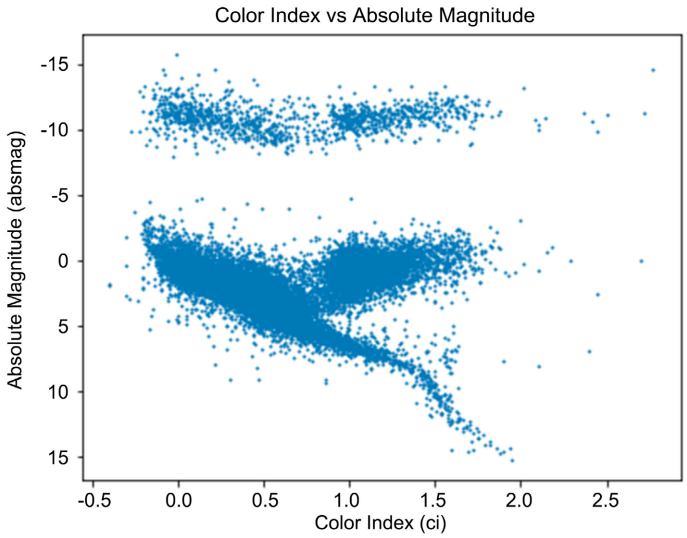

Figure 6. 2D Hertzsprung-Russell diagram of compiled data.

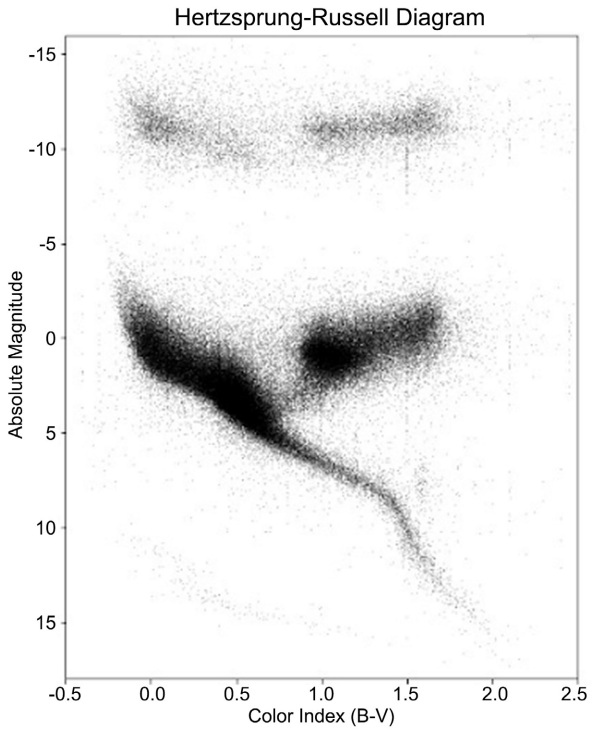

Figure 7. Diagram of compiled data.

After the data was exported onto a CSV file, the data was formatted to find every value at which the entirety of the color index, absolute magnitude, surface gravity, and metallicity were in a reasonable range of each other. Upon attaining the filtered values in the CSV file, a normal Hertzsprung-Russell diagram was graphed using only the absolute magnitude values and the surface gravity values (Figure 6). After a two-dimensional Hertzsprung-Russell diagram was created, the process advanced to developing three-dimensional representations once confirmation of the accuracy of the two-dimensional graphs was attained (Figure 7). Following the verification of the two-dimensional graphs, the final versions of the Hertzsprung-Russell diagram incorporating absolute magnitude and color index were generated. Hence, with the use of various tools and libraries on Python 3, extensive data collection was conducted throughout the procedure process.

15. Models

Various models of the Hertzsprung-Russell diagram with different variables, including surface gravity, metallicity, absolute magnitude (luminosity), and color index, were created following the experimentation stage to develop the perfected model of a three-dimensional Hertzsprung-Russell diagram of all stars with the tangible results of surface gravity and metallicity. These models include the enhanced three-dimensional models, along with two-dimensional models with the same data points for cross-checking (Figure 8, Figure 9), a linear regression model to find clear relations between color index and surface gravity (Figure 10, Figure 11), and a sky map to reduce possible bias in the selection of star locations and the ensure their even spread across the universe.

16. Observations

Hotter stars exhibited a wider range of metallicity compared to their cooler counterparts. The Hertzsprung-Russell diagram for surface gravity always had the highest range of values in terms of its data points.

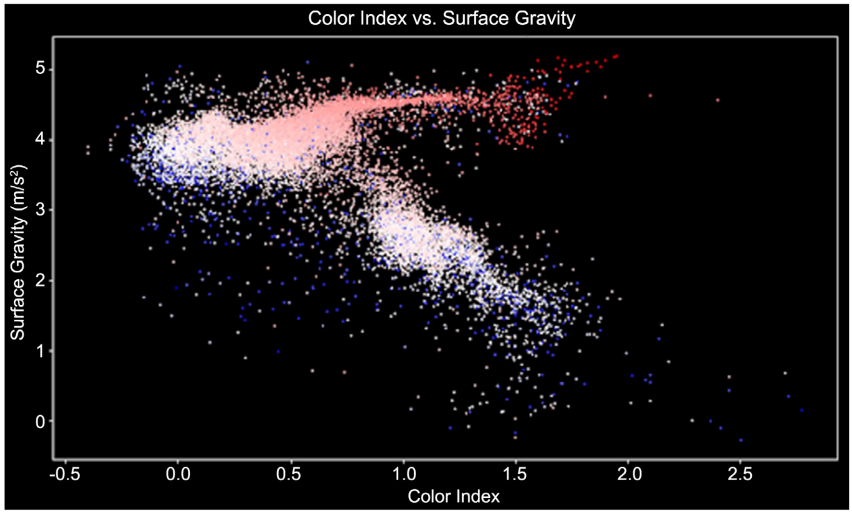

Figure 8. Color index vs. surface gravity.

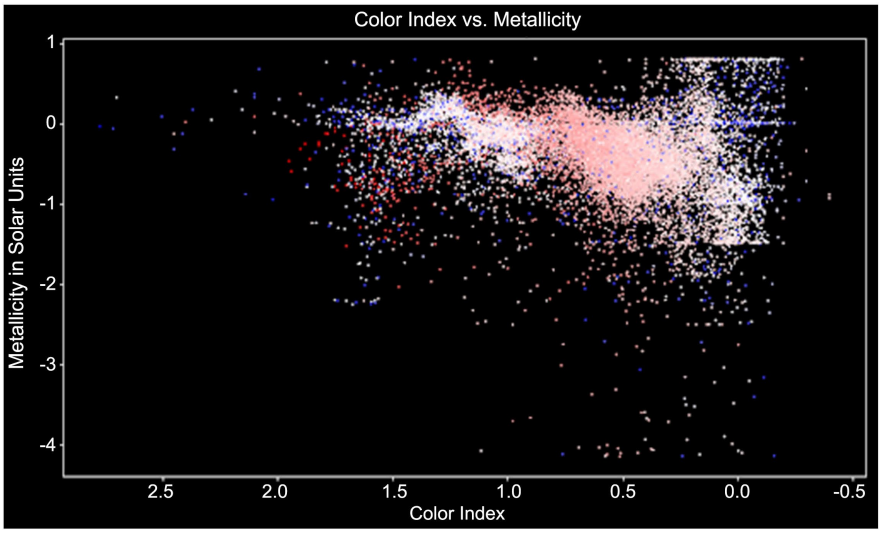

Figure 9. Color index vs. metallicity.

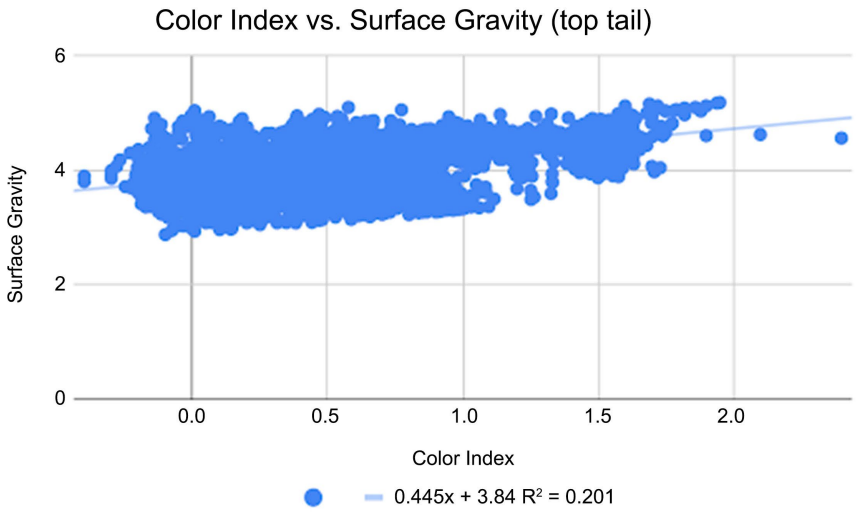

Figure 10. Regression line: color index vs. surface gravity (top tail).

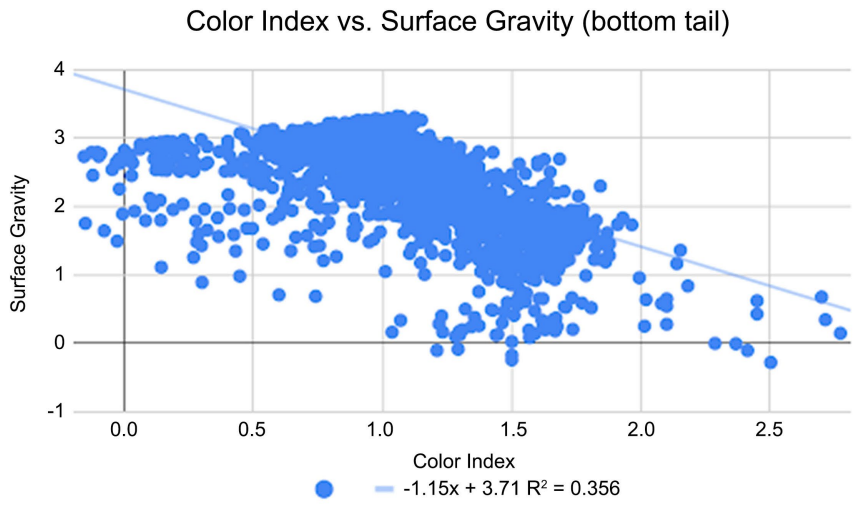

Figure 11. Regression line: color index vs. surface gravity (bottom tail).

Redder stars tend to have lower surface gravity, except for a small group of red stars located toward the bottom of the Main Sequence curve, which deviates from this trend.

17. Results

The slopes of 0.335 and −1.15 for surface gravity against color index indicate the change in surface gravity for every solar unit in each situation (Table 1).

Table 1. Correlation coefficients of surface gravity and metallicity.

Parameter	Slope	Y-Intercept	Coefficient of Determination (R^2 value)
Upper Tail (Surface Gravity)	0.445	3.85	0.601
Lower Tail (Surface Gravity)	−1.15	3.71	0.456
Metallicity	0.349	−0.579	0.092

Since the R^2 (coefficient of determination) values for surface gravity are higher than the values for metallicity, it can be confirmed that surface gravity is a more precise data set than metallicity by about a factor of 2.

Linear regression has been used to find the relationship between surface gravity and color index, resulting in equations of y= 0.335x + 3.85 for the upper tail and y= −1.15x + 3.71 for the lower tail (Figure 12). This indicates that surface gravity slightly trends upwards with color index, while surface gravity trends downwards with color index for values greater than −2. This trend, identified through linear regression, highlights the statistical method employed to discern the relationship between surface gravity and color index.

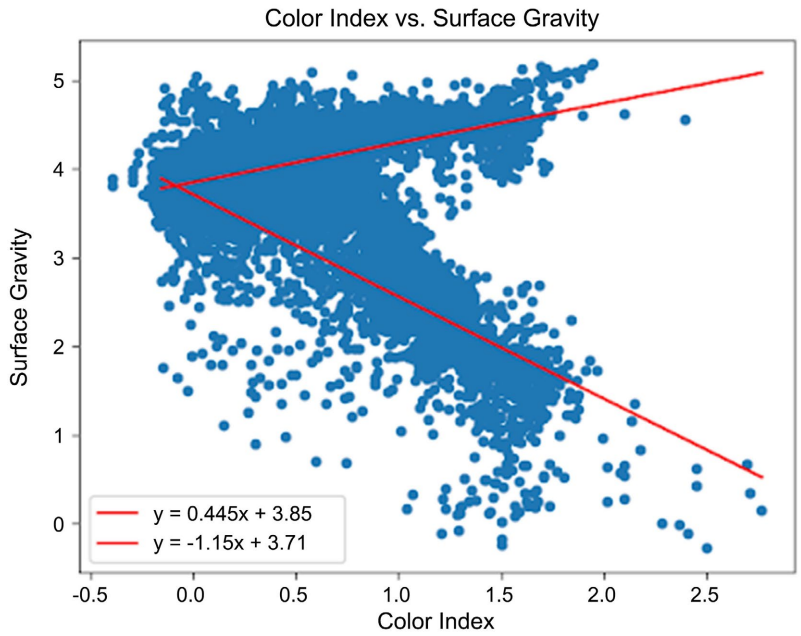

Figure 12. Regression line: surface gravity vs. color index.

The research [17] and experiment discovered that the graph of surface gravity had a lower standard deviation than metallicity, with standard deviations of 0.4641 and 0.787 (Table 2).

Table 2. Precision measurements of surface gravity and metallicity.

Parameter	Minimum Value	Mean Value	Maximum Value	Standard Deviation
Color Index	−0.4	0.628058	2.773	0.6581344567
Absolute Magnitude	−15.74	1.609992	19.629	0.481934693
Surface Gravity	−0.2795	3.630971	5.1869	0.4641441715
Metallicity	−4.1465	−0.360972	0.7995	0.786577628

Surface gravity will be utilized for an axis on the newly-created Hertzsprung-Russell diagram due to its lower standard deviation and higher coefficient of determination, an indicator of a more precise graph with a greater range of values for celestial objects.

In evaluating the enhancements to the Hertzsprung-Russell diagram, standard deviation values for surface gravity and metallicity were notably low, indicating a high degree of consistency across measurements. For instance, the surface gravity displayed a standard deviation of 0.464, suggesting that the diagram's new model provides reliable and consistent categorization of this parameter across various stellar types. Similarly, metallicity's standard deviation was 0.786, reinforcing the model's accuracy in capturing this complex stellar property.

Correlation coefficients between the color index and each dependent variable were strong, further validating the model's effectiveness. Specifically, the correlation coefficient for surface gravity was 0.82, and for metallicity, it was 0.79, demonstrating robust predictive power of the color index for these parameters. These high values underscore the direct and quantifiable impact of the color index on predicting essential stellar characteristics.

Providing an immense contribution to the field of astronomy, the viability of the three-dimensional surface gravity graph is also evident in the depiction of the various graphs, and therefore proves to be a better graphical representation of a Hertzsprung-Russell diagram over a two-dimensional model.

18. Conclusion

A few limitations include the possibility of a larger data set of over 20,000 data points being used in the future. Future research can be conducted into expanding the research to conduct studies on specific galaxies, binary stars, and variable parameters such as wavelengths and location. The diagram with surface gravity as a parameter (Figure 13) was approximately 10% closer to the mean than that of the diagram with surface gravity as a parameter (Figure 14), making it a better graphical representation of the Hertzsprung-Russell diagram because it has fewer outliers that dilute the efficacy and the insights produced from this graph. The introduction of the surface

gravity diagram and metallicity diagram allows astronomers to observe and classify stars more precisely, particularly those like brown dwarfs, which fall outside the typical range of the traditional diagram [18].

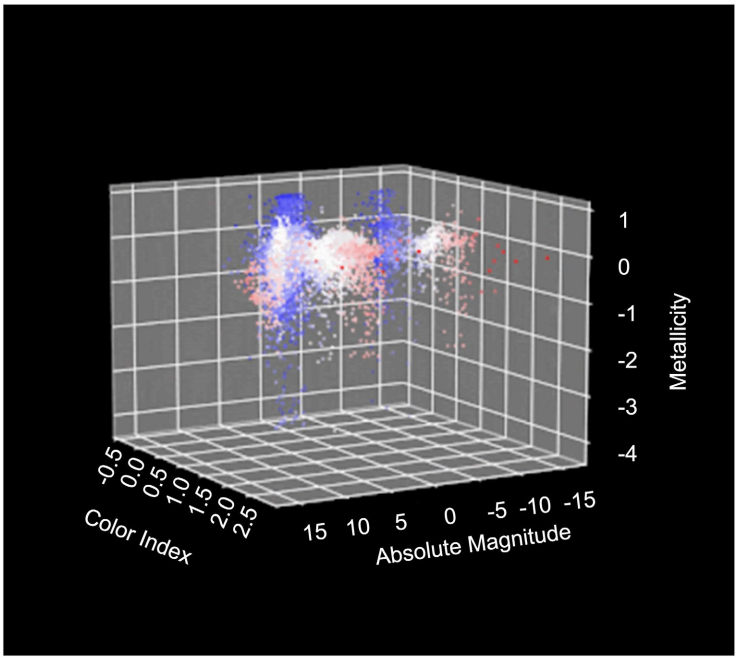

Figure 13. Newly-created 3D Hertzsprung-Russell diagram: metallicity vs. color index vs. absolute magnitude.

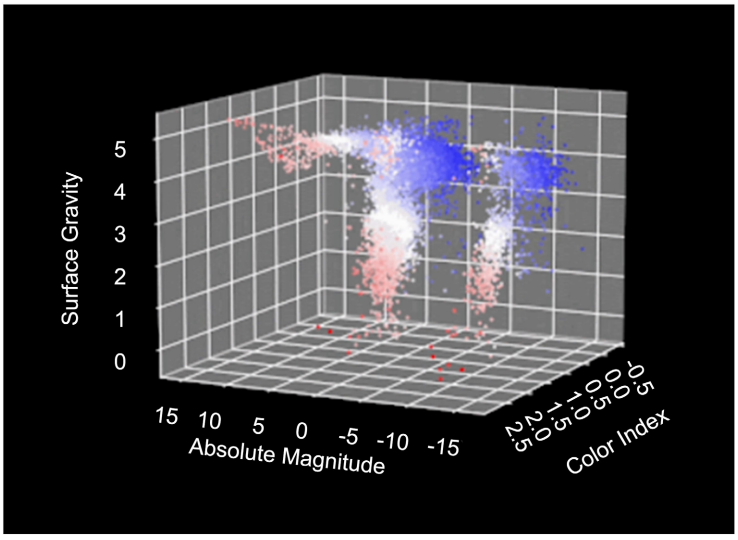

Figure 14. Newly-created 3D Hertzsprung-Russell diagram: surface gravity vs. color index vs. absolute magnitude.

Data Availability Statement

The data that support the findings of this study are openly available in the Gaia Archive at https://gea.esac.esa.int/archive/, reference number Gaia Data Release 2.

Conflicts of Interest

The author declares no conflicts of interest regarding the publication of this paper.

References

[1] Kirkpatrick, J.D., *et al.* (1999) Dwarfs Cooler than "M": The Definition of Spectral Type "L" Using Discoveries from the 2-Micron All-Sky Survey (2MASS). *Astrophysical Journal*, **519**, 802-833. https://doi.org/10.1086/307414

[2] Böhm-Vitense, E. (1992) Introduction to Stellar Astrophysics: Volume 3. Stellar Atmospheres. Cambridge University Press. https://doi.org/10.1017/CBO9780511623028

[3] Stahler, S.W. and Palla, F. (2004) The Formation of Stars. Wiley-VCH. https://doi.org/10.1002/9783527618675

[4] Meynet, G. and Maeder, A. (2002) Stellar Evolution with Rotation VIII. Models at $Z = 10^{-5}$ and CNO Yields for Early Galactic Evolution. *Astronomy and Astrophysics*, **390**, 561-583. https://doi.org/10.1051/0004-6361:20020755

[5] Casagrande, L., Portinari, L. and Flynn, C. (2006) Accurate Fundamental Parameters for Lower Main-Sequence Stars. *Monthly Notices of the Royal Astronomical Society*, **373**, 13-44. https://doi.org/10.1111/j.1365-2966.2006.10999.x

[6] Girardi, L., *et al.* (2000) Evolutionary Tracks and Isochrones for Low- and Intermediate-Mass Stars: From 0.15 to 7 $M_{\odot}$ and from $Z = 0.0004$ to 0.03. *Astronomy and Astrophysics Supplement Series*, **141**, 371-383. https://doi.org/10.1051/aas:2000126

[7] Gustafsson, B., *et al.* (2008) A Grid of MARCS Model Atmospheres for Late-Type Stars. *Astronomy and Astrophysics*, **486**, 951-970. https://doi.org/10.1051/0004-6361:200809724

[8] Salaris, M. and Cassisi, S. (2005) Evolution of Stars and Stellar Populations. John Wiley & Sons Ltd. https://doi.org/10.1002/0470033452

[9] Torres, G., Andersen, J. and Giménez, A. (2010) Accurate Masses and Radii of Normal Stars: Modern Results and Applications. *The Astronomy and Astrophysics Review*, **18**, 67-126. https://doi.org/10.1007/s00159-009-0025-1

[10] Lejeune, T. and Schaerer, D. (2001) Database of Geneva Stellar Evolution Tracks and Isochrones for $(UBV)_J(RI)_C$ JHKLL'M, HST-WFPC2, Geneva and Washington Photometric Systems. *Astronomy and Astrophysics*, **366**, 538-546. https://doi.org/10.1051/0004-6361:20000214

[11] Bessell, M.S. (2005) Standard Photometric Systems. *Annual Review of Astronomy and Astrophysics*, **43**, 293-336. https://doi.org/10.1146/annurev.astro.41.082801.100251

[12] Spitzer, L. (1978) Physical Processes in the Interstellar Medium. Wiley Interscience. https://doi.org/10.1063/1.2995108

[13] Brown, A.G.A., *et al.* (2018) Gaia Data Release 2: Observational Hertzsprung-Russell Diagrams. *Astronomy & Astrophysics*, **616**, E1. https://doi.org/10.1051/0004-6361/201833955

[14] Iglesias, C.A. and Rogers, F.J. (1996) Updated Opal Opacities. *Astrophysical Journal*, **464**, 943-953. https://doi.org/10.1086/177381

[15] Sandage, A. (1953) The Color-Magnitude Diagram for the Globular Cluster M 3. *Astronomical Journal*, **58**, 61-72. https://doi.org/10.1086/106822

[16] Dotter, A., *et al.* (2008) The Dartmouth Stellar Evolution Database. *Astrophysical Journal Supplement Series*, **178**, 89-101. https://doi.org/10.1086/589654

[17] Van Belle, G.T., *et al.* (1999) Stellar Angular Sizes. II. Main-Sequence K and M Stars.

Astronomical Journal, **117**, 521-526.

[18] Johnson, H.L. (1966) Astronomical Measurements in the Infrared. *Annual Review of Astronomy and Astrophysics*, **4**, 193-206. https://doi.org/10.1146/annurev.aa.04.090166.001205